

MS # EN-08-0361, Accepted Version Somm et al.

Prenatal Nicotine Exposure Alters Early Pancreatic Islet and Adipose Tissue Development with Consequences on the Control of Body Weight and Glucose Metabolism Later in Life

by

Emmanuel Somm¹, Valérie M. Schwitzgebel¹, Delphine M. Vauthay¹, Emily J. Camm¹,
Chang Y. Chen², Jean-Paul Giacobino³, Stéphane V. Sizonenko¹, Michel L. Aubert¹,
Petra S. Hüppi¹

¹Department of Pediatrics, Geneva University Hospitals, 1211 Geneva 14, Switzerland

²Department of Radiation Oncology, Beth Israel Deaconess Medical Center, Harvard Medical School, Boston MA 02215

³Department of Cell Physiology and Metabolism, University Medical Center, 1 rue Michel-Servet, 1211 Geneva 4, Switzerland

Running title: Prenatal nicotine and metabolic disorders

Keywords: Nicotine, pancreatic islet, adipocyte, obesity, insulin resistance

DISCLOSURE STATEMENT: The authors have nothing to disclose

Corresponding author:

Dr. E. Somm, Department of Pediatrics, Geneva University Hospitals, 1211 Geneva 14, Switzerland

Phone: (41 22) 382 45 69

Fax: (41 22) 382 43 15

Email: emmanuel.somm@medecine.unige.ch

ABSTRACT

Despite medical advice, 20% to 30% of female smokers continue to smoke during pregnancy. Epidemiological studies have associated maternal smoking with increased risk of obesity and type-2 diabetes in the offspring. In the present study, we investigated the impact of prenatal nicotine exposure (3mg/kg in Sprague–Dawley rats via osmotic Alzet minipumps) on the early endocrine pancreas and adipose tissue development in rat pups before weaning. Body weight, fat deposition, food intake and food efficiency, cold tolerance, spontaneous physical activity, glucose utilization and insulin sensitivity were also examined at adulthood. Prenatal nicotine exposure led to a decrease in endocrine pancreatic islet size and number at 7 days of life (PND7) which corroborates with a decrease in gene expression of specific transcription factors such as Pdx-1, Pax-6, Nkx6.1 and of hormones such as insulin and glucagon. The prenatal nicotine exposure also led to an increase in epididymal white adipose tissue (eWAT) weight at weaning (PND21), and marked hypertrophy of adipocytes, with increased gene expression of proadipogenic transcription factors such as C/EBP- α , PPAR- γ and SREBP-1C. These early tissue alterations led to significant metabolic consequences, as shown by increased body weight and fat deposition, increased food efficiency on high fat diet, cold intolerance, reduced physical activity, glucose intolerance combined with insulin resistance observed at adulthood. These results prove a direct association between fetal nicotine exposure and offspring metabolic syndrome with early signs of dysregulations of adipose tissue and pancreatic development.

INTRODUCTION

Obesity and insulin resistance represent a growing public health concern in both industrialized and developing countries. This rapid outbreak cannot only be explained by genetic predisposition. Other causes related to nutrition, changes in physical activity or environmental modifications could be involved. Over the last few decades, there have been accumulating evidences that the risk of developing chronic diseases in adulthood is highly influenced by environmental factors acting early in life which modify developmental plasticity. Initially, the concept of "fetal origin of adult diseases" suggested that a mismatch between fetal expectation of the postnatal environment and actual postnatal environment could contribute to later adult disease risk (1). For example, maternal protein deficiency or undernutrition, which limit fetal growth leading to a low birth weight, predispose to obesity and insulin resistance at adulthood (2, 3), especially when postnatal nutrition is highly caloric. In our modern society, however, poor food availability during pregnancy is not a widely limiting factor for fetal development. Voluntary or passive exposure to chemical pollutants is more relevant to our modern way of life. In fact, despite medical advice, more than 10% of all pregnant women continue smoking during gestation (4, 5). Initially, Williams et al. showed that fetal body fat proportion was

significantly higher in embryos exposed to nicotine compared with controls (6). Recently, numerous epidemiological studies have indicated that there is an increased risk of obesity in children born to women who smoked during pregnancy (7, 8). Very recent experimental work in rodents confirmed the direct implication of perinatal exposure to nicotine on further metabolic outcome without eluding the involved mechanisms. First, Gao et al. showed that perinatal exposure to nicotine resulted in increased postnatal body weight, fat pad weight and altered function of the perivascular WAT (9). Thereafter, Holloway et al. demonstrated that perinatal nicotine exposure also resulted in increased pancreatic β -cell apoptosis at birth and dysglycemia at adulthood (10). Finally, a recent report by Bruin et al., which studied the windows of susceptibility to nicotine exposure, concluded that only continued exposure to nicotine from conception through lactation results in permanent β -cell loss and subsequent impaired glucose tolerance, indicating that alteration by nicotine occurs both *in utero* and during lactation in rodents (11). Moreover, Levin et al. suggested that prenatal nicotinic overload blunts sympathetic responsiveness, leading to peripheral and central underactivity of the noradrenergic system (12).

The phenotype of perinatal nicotine exposure is therefore complex and still poorly understood. In order to better understand the main mechanism(s) of the observed alterations

and to elucidate primary vs secondary programming effects, we performed a systematic analysis, studying, in particular, body weight from birth, pancreatic islet and adipose tissue development in the early postnatal period, response to high fat diet, food intake and food efficiency, energy expenditure, cold adaptation, physical activity, glucose tolerance and insulin sensitivity at adulthood in Sprague–Dawley rats exposed to nicotine (3mg/kg via osmotic minipumps) during their uterine life.

METHODS

Animals

All experimental protocols were approved by the "State of Geneva Veterinary Office" (Geneva, Switzerland). Virgin female (275-300g) and male (300-325g) Sprague-Dawley OFA rats (Charles River Laboratories, France) were used for breeding and housed under specific pathogen-free conditions in an environmentally-controlled clean room at the School of Medicine animal facilities (Medical Center University, University of Geneva). The day that sperm-positive smears were obtained was declared day 0 of gestation. Pregnant rats were housed individually under standard conditions (12/12 h light, dark cycle), with free access to food and water.

Surgical procedures and nicotine exposure

Starting on day 4 of gestation, nicotine (nicotine hydrogen tartrate, Sigma Aldrich, Buchs, Switzerland) or saline was infused subcutaneously via Alzet osmotic minipumps (Charles River Laboratories, France). Pumps were filled with a nicotine solution, at a concentration calculated to deliver 3mg/kg/day of nicotine during 14 days. Consequently, we only studied nicotine exposure during pregnancy. All pumps were incubated in physiological saline for 4 h at 37°C before implantation. Activated pumps were then implanted subcutaneously (along the midline at the midthoracic level) under isoflurane anesthesia. For all experiments, only male pups exposed *in utero* to nicotine were utilized.

Detection of nicotine metabolites in blood of gestating dams

Quantitative determination of cotinine and other principal metabolites of nicotine in serum

of control and nicotine-exposed pregnant rats were determined with a solid-phase competitive chemiluminescent Immunoassay (IMMULITE, Diagnostic Products Corporation, Los Angeles, USA) at days 1, 5 and 19 of gestation (G1, G5 and G19).

Histological examination of pancreas and adipose tissue

Pancreases of 5 to 6 rats per group, at 7 days of age (PND7) were fixed in Bouin's solution, embedded in paraffin and 5 µm sections were stained with aldehyde fuchsine. Eight sections of each pancreas were analyzed using a personalized program in MetaMorph® Imaging System (Meta Imaging Software, Molecular Devices Corporation, Pennsylvania, U.S.A). This program determines the total area of pancreatic tissue, the total area of Langerhans islets, the number of islets and their size. For number and size determination, only islets bigger than 300 µm² were used for calculation. For the immunohistochemical staining of the survivin protein, formalin-fixed, paraffin-embedded tissue blocks were sectioned to 5 µm and baked overnight at 60°C. The slides were deparaffinated with xylene and rehydrated through graded alcohols and endogenous peroxidase activity was blocked by a 15-minute treatment with 3% hydrogen peroxide. Antigen retrieval was performed by heating the slides for 10 minutes in a 20 mmol/L concentration of citrate buffer (pH 6.0). The sections were processed by an indirect immunoperoxidase method, using a polyclonal rabbit anti-survivin antibody (kind gift of Pr K.R. Shroyer) at 1.0 µg/mL with peroxidase-labeled goat anti-rabbit immunoglobulin secondary antibody. Subsequently, the sections were developed using 3, 3'-diaminobenzidine, counterstained with hematoxylin, dehydrated in graded alcohols and finally coverslipped before photographs were taken.

Epididymal WAT of 5 to 6 rats per group, at 21 days of age, were fixed in a paraformaldehyde solution, embedded in paraffin and 5 µm sections were stained with hematoxylin/eosin. The morphometric measurements were performed on 6 serial sections taken every 100 µm for each animal. Fifty to one hundred adipocytes were measured in each section (300-600 cells analyzed in total per rat) and the area of each adipocyte was determined using the Image J software

(Rasband W.S, ImageJ, NIH, Bethesda, Maryland, USA).

Islet isolation

Islets of Langerhans were isolated from the pancreases of rats at 7 days of age by collagenase type V (Sigma Aldrich, Buchs, Switzerland) digestion and purification on a Histopaque® 1077 (Sigma Aldrich, Buchs, Switzerland) gradient. The pancreas was immediately excised and cut in small parts in Hanks solution and placed in a conical tube containing 5 mL of the collagenase and Hanks solution. The resected pancreas was incubated in a 37°C water bath for 7 minutes. The digestion was stopped by addition of Hanks/BSA on ice. The pancreatic tissue was centrifuged several times and the undigested fragments were carefully removed. After washing with Hanks solution, the tissue was concentrated into a pellet. The tissue pellet was resuspended in Ficoll 1.077 mg/mL. After centrifugation at 2500 rpm for 20 minutes, islets were harvested from the interface between the layers. After washing, islets were concentrated into pellets and immediately used for RNA extraction.

RNA preparation and mRNA quantification

Total RNA from islets was extracted using the RNeasy Mini Kit® according to the manufacturer's protocol (Qiagen, Basel, Switzerland). Total RNA from eWAT was prepared using the Trizol reagent (Invitrogen, Basel, Switzerland), according to manufacturer's instructions. For pancreatic islets and eWAT, respectively one and five micrograms total RNA were reverse-transcribed using 800 units of Moloney murine leukemia virus reverse transcriptase (Invitrogen, Basel, Switzerland), in the presence of 0.3 units/μl RNAsin (Promega Corp, Madison, WI), 7.5 μM of random primers (oligo(dN)6), 1.2 mM dNTP and 12 μM of DTT. The expression of the cDNAs for rat HNF-3β (foxa2), Pdx-1, Pax-6, Nkx6.1, insulin, glucagon, kir6.2, glut 2, glucokinase, survivin for pancreatic islet and C/EBP-α, PPAR-γ, SREBP-1C, GATA-2, aP2, adipon, leptin, resistin, apelin, LPL for the adipose tissue were determined by quantitative real-time PCR using an ABI 7000 Sequence Detection System (Applied Biosystems, Rotkreuz, Switzerland) and were normalized using the housekeeping gene 36B4. PCR products were

quantified using the SYBR Green Core Reagent kit (Applied Biosystems, Rotkreuz, Switzerland) and results are expressed in arbitrary units (A.U). Primers were designed using the Primer Express software (Applied Biosystems, Rotkreuz, Switzerland). The sequence of the primers used is provided in Table 1.

Pancreatic insulin content and insulinemia

Total pancreas, frozen in liquid nitrogen, were pulverized, resuspended in cold acid ethanol, and left at 4°C for 48 h, with sonication every 24 h. Insulin content in the acid ethanol supernatant as well as insulin content in blood samples were determined with a rat insulin RIA kit from Linco (Labodia S.A., Yens, Switzerland).

Diet, food intake and body weight measurement

At weaning (PND21), prenatally nicotine-exposed rats and controls were fed ad libitum either a standard chow diet (where 7% of the calories were derived from fat, 76% from carbohydrates and 17% from proteins) or a high fat diet (40% of the calories were derived from fat, 43% from carbohydrates and 17% from proteins). Metabolizable energy of standard chow and high fat diet were 2.6 and 4.3 kcal/g, respectively. Body weight and food intake was measured weekly from week 4 to 18.

Calorimetry and physical activity measurements

Analyses for indirect calorimetry, spontaneous activity and circadian food behavior were realized on prenatally nicotine-exposed and control 18-week-old rats using the LabMaster system (TSE Systems GmbH, Berlin, Germany) in the Small Animal Phenotyping Facility (CMU, University of Geneva, Geneva), under standard laboratory conditions (22 ± 1°C ambient temperature, light-dark cycle of 12/12 h, ad libitum food and water). The calorimetry system is an open-circuit determining O₂ consumption (ml/kg/h), CO₂ production (ml/kg/h), respiratory exchange rate (RER = VCO₂ / VO₂, where V is volume). Detection of animal location and movements are monitored by infrared sensor pairs arranged in strips for horizontal activity, discriminating between ambulatory and fine movements. The LabMaster also consists in a combination of highly sensitive feeding sensors responsible for

automated online measurements. All of these parameters can be measured continuously and simultaneously for all animals studied. Before recording, animals were allowed a 4-day acclimatization period in the training cages. Measurements were realized thereafter over two successive 24 h periods.

Cold exposure

Control and prenatally nicotine-exposed rats fed with a standard rat chow diet once weaned were used for an acute cold exposure test at 15 weeks of age. Rats were individually caged supplied with a minimum of wood shavings at 4°C for 6 h with free access to food and drinking water. Rectal temperature was monitored every 2 h in the 4°C environment.

Glucose tolerance test and insulin tolerance test

For the glucose tolerance test, 26-week-old rats prenatally exposed to nicotine or saline were fasted 16 h before receiving an i.p. injection containing 1.5 mg glucose per g of body weight. For the insulin tolerance test 10 days later, the same rats were fasted for 3 h prior to i.p. injection with 1 mU human recombinant insulin (Actrapid, Novo Nordisk, Bagsvaerd, Denmark) per g of body weight. Blood samples were collected by tail puncture for immediate glycemia measurement using a glucometer (Glucotrend Premium, Roche Diagnostics, Rotkreuz, Switzerland) and other samples were collected in heparin-coated tubes, placed on ice, centrifuged and plasma was frozen for insulin dosage with RIA kits from Linco (Labodia S.A., Yens, Switzerland).

Statistics

Results are expressed as mean \pm SEM. The unpaired Student's t-test and repeated-measures one-way analysis of variance (ANOVA) were used when appropriate for comparison between groups of rats. These tests were performed with SYSTAT 10.01 (SPSS, Chicago, IL). A p value of < 0.05 was considered statistically significant.

RESULTS

Increased nicotine metabolite levels in pregnant rats

The weight gain, food intake and drinking volume during gestation of nicotine-exposed rats were not significantly different from those of controls despite the increase in blood nicotine metabolite levels. In fact, one day after implantation of the subcutaneous osmotic minipumps, the levels of circulating metabolites of nicotine, which are undetectable in control animals, rose to 281 ± 18 ng/ml and remained elevated (252 ± 12 ng/ml) until gestational day 19 before parturition of pups (Figure 1).

Increased body weight in prenatally nicotine-exposed rats

Unlike humans and some animal species, birth body weight of pups exposed *in utero* to nicotine is not altered in our model, both in males (5.85 ± 0.06 g for prenatally nicotine-exposed compared to 5.82 ± 0.05 g for control animals, $n=132-139$ animals per group, $p=0.76$) and in females (5.54 ± 0.05 g for prenatally nicotine-exposed compared to 5.56 ± 0.06 g for control animals, $n=145-159$ animals per group, $p=0.77$) (Figure 2A). However, at postnatal day 7 (PND7), prenatally nicotine-exposed rats start gaining more weight than controls. At weaning (PND21), prenatal nicotine exposure resulted in a 7% increase in body weight in male rats as compared to controls ($p<0.05$) (Figure 2A).

Increased white fat and adipogenesis in prenatally nicotine-exposed rats

Since previous studies have indicated that adult rats exposed perinatally to nicotine have heavier perivascular and abdominal fat pads, we weighed adipose tissue deposition at weaning (PND21) in male pups. As shown in Figure 2B, male pups exposed to nicotine during their uterine life present heavier epididymal white adipose tissue (eWAT) and lighter brown adipose tissue (BAT) than control pups whereas kidney and liver weights were unaffected. To determine whether the early increase in white adipose tissue mass observed in prenatally nicotine-exposed rats was associated with an increase in number of adipocytes (hyperplasia) or an increase in size of adipocytes (hypertrophy), we performed

morphometric analysis on histological sections of eWAT (Figure 3A). Quantitative analysis of these sections (Figure 3B) showed that at this early age the adipocytes were $38 \pm 5\%$ larger in prenatally nicotine-exposed rats ($1074 \pm 42 \mu\text{m}^2$) than in controls ($779 \pm 27 \mu\text{m}^2$) ($p < 0.01$), suggesting that adipose tissue enlargement in rats prenatally exposed to nicotine is due to excessive levels of differentiation and lipid storage rather than to increased preadipocyte recruitment. This early adipocyte hypertrophy in prenatally nicotine-exposed rats is confirmed by the observed increase in gene expression levels of C/EBP- α , PPAR- γ , SREBP-1C, aP2 and adipsin, classical transcription factors and markers involved in the adipocyte differentiation process (Figure 3C). No change in gene expression levels of GATA-2 or KLF-5 was detected. Moreover, the mRNA expression of some adipokines was altered in prenatally nicotine-exposed rats. For example, leptin mRNA levels were increased 9.1 ± 1.6 fold, resistin 3.3 ± 0.5 fold and apelin 4.2 ± 0.5 fold in eWAT in prenatally nicotine-exposed animals (data not shown). TNF- α , IL-6, PAI-1 and visfatin gene expression remained unchanged (data not shown), demonstrating that adipose tissue gene expression modifications were specific and not related to a systemic tissue inflammation. The lipogenesis-promoting enzyme lipoprotein lipase (LPL) mRNA level was also increased 2.08 ± 0.26 fold in eWAT in prenatally nicotine-exposed animals.

In summary, these results show that prenatal nicotine exposure results in higher body weight and fat content at weaning mainly due to hypertrophy of adipocytes associated with an increased expression of genes involved in adipocyte differentiation and genes coding for adipocyte secreted factors.

Altered pancreatic development in prenatally nicotine-exposed rats

In order to evaluate the impact of prenatal nicotine exposure on the endocrine pancreas development, morphometric analysis of pancreas were performed at PND7 (Figure 4). The ratio of endocrine to whole pancreas area was significantly reduced in prenatally nicotine-exposed animals ($1.20 \pm 0.17\%$) compared to control animals ($1.74 \pm 0.13\%$) (Figure 4A, top panel) ($p < 0.05$). This reduction in the endocrine pancreas was related to a concomitant decrease in mean islet size (1581

$\pm 86 \mu\text{m}^2$ for prenatally nicotine-exposed compared to $1867 \pm 80 \mu\text{m}^2$ for control animals, $p < 0.05$) (Figure 4A, middle panel) and the number of islets (63 ± 3 islets/section for prenatally nicotine-exposed compared to 80 ± 5 islets/section for control animals, $p < 0.05$) (Figure 4A, bottom panel).

To extend this histological analysis, gene expression of different transcription factors involved in pancreatic cell differentiation was analyzed (Figure 4B). Despite no change in HNF-3 β (also named *foxa2*) gene expression, a transcription factor which triggers both endocrine and exocrine pancreas development and controls insulin secretion in mature β -cells (13), a reduction in expression of different transcription factors specific for endocrine cells was observed, such as for Pdx-1 (specific for β -cells after birth), Pax-6 (expressed in all mature endocrine cells) and Nkx6.1 (specific for β -cells) in the islets of prenatally nicotine-exposed pups. In accordance with this reduction in the main endocrine transcription factor expression, we noticed significant reduction in both insulin and glucagon mRNA levels in the prenatally nicotine-exposed pups. At the protein level, insulin content in the pancreas of prenatally nicotine-exposed rats showed a trend to decreased levels ($732 \pm 36 \mu\text{g}$ of insulin per gram of pancreas) when compared to control rats ($883 \pm 56 \mu\text{g}$ of insulin per gram of pancreas) ($p = 0.06$, $n = 5-6$ animals per group, data not shown). Expression of Kir6.2 (a subunit of the K⁺/ATP channels), glut 2 (glucose transporter type 2) and glucokinase (metabolic sensor involved in the regulated release of insulin) mRNA were also all significantly decreased in pancreatic islets from prenatally nicotine-exposed rats. Finally, a decrease in gene expression for survivin (also named IAP for Inhibitor of Apoptosis), which plays a role in endocrine pancreatic remodeling and islet homeostasis, was detected in prenatally nicotine-exposed animals. The mRNA downregulation of the survivin anti-apoptotic factor was also confirmed by immunohistochemical assessment (Figure 4C). Indeed, the immunolabeling of the survivin protein appears weaker in prenatally nicotine-exposed pups (right panel) as compared to controls (left panel). Survivin is specifically located on the periphery of islets, in the α -cells, at this stage of development.

In summary, these results show that prenatal nicotine exposure results in altered endocrine pancreas in rat pups due to reduction in size and number of Langerhans islets associated with a decreased expression of genes involved in α and β -cells differentiation process.

Increased body weight curve and fat pads in prenatally nicotine-exposed rats

Body weight of prenatally nicotine-exposed rats was increasing more rapidly than their respective controls, both when fed chow or a high fat diet (HFD) after weaning ($p < 0.05$) (Figure 5A). Surprisingly, the body weight curve of prenatally nicotine-exposed animals fed with the chow diet (started at weaning) catches up with the curve of unexposed animals fed with a HFD (started at weaning), indicating that prenatal nicotine exposure predisposes to a comparable weight gain as consumption of a HFD.

At 20 weeks of age, eWAT mass of prenatally nicotine-exposed animals is heavier than those of control animals (4.6 ± 0.4 g for nicotine versus 3.5 ± 0.4 g for controls, $p < 0.05$) and this observation is exacerbated in animals fed a HFD (9.5 ± 0.9 g for nicotine versus 6.2 ± 0.5 g for controls, $p < 0.02$) (data not shown). Retroperitoneal WAT (rpWAT) mass of prenatally nicotine-exposed animals under HFD since weaning is also significantly heavier than those of control animals (13.2 ± 1.6 g for nicotine versus 8.8 ± 1 g for controls, $p < 0.05$) (data not shown).

Unchanged food intake but increased food efficiency during HFD in prenatally nicotine-exposed rats

To investigate whether appetite control is modified by prenatal nicotine exposure, we measured both long term energy intake under chow and HFD and daily circadian food intake. During the 14 consecutive weeks of measurement, despite caloric hyperphagia induced by HFD in control and prenatally nicotine-exposed animals, no impact of prenatal nicotine exposure on energy intake was detected. On chow diet, prenatally nicotine-exposed animals ingested 5862 ± 151 kcal versus 5612 ± 120 kcal for controls ($p = 0.23$) whereas on a HFD, prenatally nicotine-exposed animals absorbed 6530 ± 155 kcal versus 6783 ± 294 kcal for controls ($p = 0.47$) (Figure 5B). Prenatal exposure to nicotine did not affect post-weaning food

intake during growth, whether in standard conditions or on a high caloric diet.

When food intake was calculated relative to the increase in body weight (food efficiency) over the 14 first post-weaning weeks period, the prenatally nicotine-exposed and control rats had a similar food efficiency on chow diet (respectively 6.16 ± 0.20 and 6.29 ± 0.07 g of food/g b.w. gain/14 weeks, $p = 0.58$) but the prenatally nicotine-exposed rats needed less food to gain weight on a HFD than controls (respectively 3.76 ± 0.07 and 4.20 ± 0.16 g of food/g b.w. gain/14 weeks, $p < 0.02$) suggesting a higher storage or decreased energy expenditure (Figure 5C).

At 18 weeks of age, daily food intake on chow diet is similar in the prenatally nicotine-exposed and control rats (20.69 ± 1.15 g and 20.24 ± 0.95 g, respectively, $p = 0.76$). In the same way, prenatally nicotine-exposed and control rats consume the same proportion of their daily ration during the nocturnal period ($69 \pm 3\%$ and $71 \pm 2\%$, respectively, $p = 0.55$) (data not shown).

Basal energy expenditure is not altered at adult age in prenatally nicotine-exposed rats

We carried out indirect calorimetry measurements to investigate whether the predisposition to gain weight was caused by decreased energy expenditure in prenatally nicotine-exposed rats. No difference was observed in oxygen consumption, during the lights-on period (514 ± 23 ml/h/kg for nicotine versus 480 ± 11 ml/h/kg for controls, $p = 0.23$) as well as during the dark period (602 ± 13 ml/h/kg for nicotine versus 601 ± 13 ml/h/kg for controls, $p = 0.97$) (data not shown).

The respiratory exchange ratio was identical between prenatally nicotine-exposed and control rats, either during the lights-on period (0.89 ± 0.01 for nicotine and 0.89 ± 0.01 for controls, $p = 0.95$) or the dark period (0.96 ± 0.01 for nicotine and 0.96 ± 0.01 for controls, $p = 0.92$), indicating that the two groups of animals were predominantly using fatty acids in store during the lights-on period and carbohydrates from alimentation during the dark period (data not shown), with no difference in energy expenditure.

Increased short-term cold sensitivity at the adult age in prenatally nicotine-exposed rats

Acute cold exposure of animals (at 4°C) is a well known method used to investigate non

shivering thermogenesis in rodents. After a 2 h cold-exposure, a length of time which corresponds to shivering adaptation to cold, no change in rectal temperature was observed between control and prenatally nicotine-exposed rats (Figure 5D). However, after a 4 h cold-exposure, rectal temperature was decreased by 1.28 ± 0.17 °C in nicotine rats and only by 0.63 ± 0.14 °C in control rats ($p < 0.02$). In the same way, after a 6 h cold-exposure, rectal temperature was decreased by 1.54 ± 0.25 °C in nicotine rats and only by 0.61 ± 0.21 °C in control rats ($p < 0.02$) indicating perturbed thermogenesis due to prenatal nicotine exposure.

Decreased physical activity at the adult age in prenatally nicotine-exposed rats

Spontaneous ambulatory activity was significantly reduced in prenatally nicotine-exposed rats during the dark period, the main activity period of rodents (10549 ± 623 counts) when compared to controls (13944 ± 1465 counts, $p = 0.04$) (Figure 5E). During lights-on period there was a trend towards decreased activity in prenatally nicotine-exposed rats (3748 ± 57 counts) when compared to controls (4772 ± 523 counts, $p = 0.06$).

Glucose intolerance and insulin resistance at the adult age in prenatally nicotine-exposed rats

At 20 weeks of age, no difference in basal insulinemia (2 h after food removal) was detected between prenatally nicotine-exposed (1.07 ± 0.24 ng/ml) and control animals (0.89 ± 0.21 ng/ml, $p = 0.59$, $n = 10$, data not shown). Moreover, no correlation between body weight and insulinemia could be observed.

However, in order to determine whether early alterations in pancreatic islets and adipocytes represent an unfavourable impact on glucose homeostasis later in life, we performed glucose as well as insulin tolerance tests in 26-week-old rats. At this age, basal glycemia after 16 h of fasting was similar in control and rats prenatally exposed to nicotine (4.8 ± 0.2 and 5.0 ± 0.1 mmol/L, respectively, $p = 0.52$). Fasting insulinemia was also similar in control and nicotine rats (0.25 ± 0.07 and 0.34 ± 0.01 ng/mL, respectively, $p = 0.34$). However, circulating glucose clearance after i.p. administration was delayed in prenatally nicotine-exposed rats (Figure 6A, left panel), reflecting a decrease in glucose utilization.

This was confirmed by the increased area under the curve (AUC) in nicotine rats (1224 ± 66 mmol/L*min) as compared to control animals (968 ± 65 mmol/L*min) ($p < 0.02$) (Figure 6A, right panel). Insulin secretion during this glucose tolerance test was higher in prenatally nicotine-exposed rats (Figure 6B), suggesting that the decrease in glucose utilization is not due to a defect in insulin production and/or secretion but to an alteration of sensitivity of peripheral tissues to insulin action. To further test this hypothesis, we performed an insulin tolerance test on the same cohort of animals after 10 days of recovery. As shown in Figure 6C, left panel, blood glucose decrease was less pronounced in prenatally nicotine-exposed rats ($26 \pm 3\%$ after 30 min), than in controls ($35 \pm 3\%$ after 30 min), and the area below the curve was significantly higher in nicotine rats ($45.4 \pm 1.4\%$ of decrease*min) than in controls ($40.8 \pm 1.4\%$ of decrease*min) ($p < 0.05$) (Figure 6C, right panel), confirming a reduction in insulin sensitivity in prenatally nicotine-exposed animals. Mechanisms involved in this insulin resistance remain to be determined. Our data suggests that neoglucogenesis is not altered by prenatal exposure to nicotine. In fact, the mRNA gene expression of glucose 6 phosphatase (G6Pase) and phosphoenolpyruvate carboxykinase (PEPCK) were unchanged in the liver of prenatally nicotine-exposed as compared to control animals (data not shown).

We also studied, at adulthood, the mRNA expression of adiponectin and resistin, two major adipose-derived hormones, respectively enhancing and lowering insulin sensitivity. Adiponectin was overexpressed in eWAT of prenatally nicotine-exposed animals (2.23 ± 0.24 A.U) when compared to controls (1 ± 0.20 A.U) as was the case for resistin (2.00 ± 0.28 A.U in nicotine compared to 1 ± 0.23 A.U in control animals).

DISCUSSION

Numerous reports have described the higher prevalence of obesity and diabetes in children born to smoking women (7, 8, 14) but little explanation is proposed to explain this phenomenon. Confounding social factors are sometimes argued rather than a direct effect of nicotine or other cigarette components. In order to mimic these clinical observations, we exposed gestating Sprague-Dawley dams to nicotine via a subcutaneous osmotic minipump at a dose of 3 mg/kg/day, a practical method for continuous delivery to the pup while minimizing stress due to handling the gestating mothers. This exposure resulted in circulating nicotine metabolite levels measured in gestating females which were found to range between 250-300 ng/ml. These values are relevant as well as in regards to those found in smokers consuming daily between 10-19 cigarettes whose serum cotinine levels were comprised between 320 and 430 ng/ml (15) and to those reported in pregnant women using nicotine patches as tobacco substitutes (16), another clinical situation involving continuous nicotine exposure. In consequence, we do believe that our rat model faithfully reproduces the smoking situation and the nicotine patches utilisation in humans.

A primary direct noxious effect of prenatal nicotine exposure on endocrine pancreas development was substantiated with the ratio of endocrine to whole pancreas area being significantly reduced at PND7, due to concomitant decrease in islet size and number. This direct effect might be modulated through the nicotinic cholinergic receptors (nAChR) subunits $\alpha 2$ - $\alpha 4$, $\alpha 6$, $\alpha 7$ and $\beta 2$ - $\beta 4$ present in the rat pancreas at PND1 (17). In the present study, we demonstrated that these morphometric observations are reinforced by our finding that the gene expressions of endocrine cell specific transcription factors and of hormones are reduced. These decreases might be due to the higher level of apoptosis in the pancreatic islets of the early nicotine-exposed pups previously reported (10) and which was recently ascribed to an elevation in oxidative stress (18) and in mitochondrial pro-apoptotic pathway (19). Our present data show that the apoptotic effect produced by the prenatal nicotine exposure is not restricted to β -cells but is also effective on α -cells, as demonstrated by decreased gene expression for

glucagon. We confirm that survivin expression is restricted to α -cells at PND7 in rat pancreatic islets, as is the case in human islets after birth (20). The downregulation of the expression of survivin in the islets of prenatally nicotine-exposed pups could link nicotine and apoptosis. Regulation of survivin gene expression by nicotine seems to be cell type-dependant since in human cancer cell lines nicotine activates survivin expression (21, 22). At adulthood, no change in basal and fasting glycemia or insulinemia was observed, and these parameters failed to correlate with body weight. However, a delay in glucose clearance after an intra-peritoneal glucose tolerance test (IPGTT) was observed in prenatally nicotine-exposed animals, suggesting a decrease in glucose utilization. The same observation were made from data obtained after an oral glucose tolerance test (OGTT) (10, 11). The similar delay in glucose utilization despite the difference in route of administration (oral or i.p.) excludes that the defect in glucose homeostasis would involve gastrointestinal control of glycemia via incretin secretion. Moreover, the insulin hypersecretion observed during our IPGTT is in accordance with that previously reported during an OGTT (10). Altogether, these results suggest that the decrease in glucose utilization observed after prenatal nicotine exposure is due to an alteration of peripheral insulin sensitivity rather than to a defect in insulin production and/or secretion. Indeed, performing an insulin tolerance test (ITT), we demonstrated for the first time a decrease in insulin sensitivity in prenatally nicotine-exposed animals. In consequence, our phenotype is highly similar to the pre-diabetic situation in humans, a pathologic status associated with a decrease in β -cell mass (23) and during which hypersecretion of insulin is not sufficient to compensate for peripheral insulin resistance. Mechanisms leading to decreased insulin sensitivity in rats prenatally exposed to nicotine remain to be further elucidated. Excessive endogenous glucose production does not seem to be involved in this process, as demonstrated by absence of an up-regulation of hepatic PEPCK and G6Pase gene expression in our model.

Moreover, parallel gene overexpression of both adiponectin and resistin, two adipokines with antagonistic effects on insulin sensitivity, in adipose tissue of rats prenatally exposed to

nicotine, did not allowed to elucidate a clearly altered crosstalk between adipose tissue secretion and glucose consuming tissue in our model.

In comparison to previous data suggesting that the dysglycemia observed after nicotine exposure through gestation and lactation precedes the development of obesity (10), our study demonstrates that body weight changes appear early after prenatal nicotine exposure. In fact, we are the first to report that prenatally nicotine-exposed rats are heavier than controls at weaning on postnatal day 21 (PND21), a period which corresponds to childhood in humans. In previous studies involving other strains of animals and different doses, routes and windows of exposure, an increase in body weight in perinatally nicotine-exposed animals appeared later, at adulthood (10 weeks of age) (9). To determine whether early higher body weight induced by prenatal nicotine exposure is associated with an increase in fat mass as observed in human children, we analyzed eWAT at PND21. Pups exposed to nicotine presented an increase in eWAT of one third compared to controls. We demonstrate that this adipose tissue enlargement in pups prenatally exposed to nicotine is due to an enhanced differentiation of their adipocytes, rather than to a recruitment of their preadipocytes. This observation is important because hypertrophy of white adipose tissue could be reversed more easily than hyperplasia.

Among the numerous changes in gene expression observed in the adipose tissue of young rats prenatally exposed to nicotine, those of LPL and PPAR- γ are interesting. In fact, the overexpression of LPL raises the possibility that the breakdown and uptake of lipoprotein triglycerides into adipocytes are enhanced after prenatal nicotine exposure. Moreover, the overexpression of PPAR- γ , the key transcription factor triggering adipocyte differentiation, could be one of the initial links between early nicotine exposure and later obesity. In this way, a recent report support this observation showing that monocytes from healthy smokers present a constitutively enhanced PPAR- γ expression (24) and that PPAR- γ gene expression could be increased directly by nicotine *in vitro* (24).

In our study, the post-weaning body weight curves of prenatally nicotine-exposed rats are steeper and the different fat pad depots are greater than those of controls on chow diet, in

accordance with previous data (9). More importantly, we show with the present study that this weight gain is exacerbated when the nicotine-exposed animals are fed a HFD after weaning. This observation is relevant to the human situation in which prenatal nicotine exposure can potentiate the development of obesity in children consuming a high calorie diet.

One interesting question was to determine whether the obese phenotype, after prenatal nicotine exposure, was due to programmed changes in food intake and/or in energy expenditure later in life. In fact, it is well known that nicotine acts directly on neuropeptides involved in appetite to repress food intake (25). We found no effect of prenatal nicotine exposure on cumulative energy intake later in life between 4 to 18 weeks of age, whether on a normal chow or a HFD. Moreover, daily food intake and circadian distribution of meals were also similar in the prenatally nicotine-exposed and control animals at 18 weeks of age. Finally, we also observed that orexin gene expression was slightly reduced and CART gene expression was slightly induced at PND21 in the hypothalamus of pups prenatally exposed to nicotine (Somm. E, unpublished observations), in accordance with clinical data indicating that offspring of mothers who smoked during pregnancy were more likely to report a poor appetite independent of a number of potential confounding factors (26). All of these endpoints exclude the programming of a hyperphagic behavior after prenatal nicotine exposure.

However, we observed that prenatally nicotine-exposed rats need significantly less food than controls to gain weight on a HFD. Different factors seem to contribute to this higher food efficiency. The first one is decreased physical activity. We indeed observed a slight decrease in voluntary ambulatory activity in prenatally nicotine-exposed rats at adulthood as reported recently at a younger age (27). Altered spontaneous physical activity is also in accordance with recent reports showing that perinatally nicotine-exposed rats have significantly slower swimming speeds (28), possibly due to alterations in motor behavior related to disruptions in the mesoaccumbens dopaminergic pathway (29).

A higher food efficiency might also be related to differences in development and function of

the gastrointestinal tract. Differences in nutrient absorption and in the microbiota composition in the gut, an emerging factor contributing to the pathophysiology of obesity (30, 31), remain to be investigated in our model.

Finally, a higher food efficiency might also be due to decreased thermogenesis. We noticed that prenatally nicotine-exposed rats, unlike controls, failed to maintain their body temperature during a short-term cold exposure. Brown adipose tissue, because it contains a unique mitochondrial uncoupling protein, termed uncoupling protein-1 (UCP1), is considered as the main effector of adaptive thermogenesis in rodents (32). Cold-exposure, via a stimulation of the brown adipose tissue sympathetic nervous system and the β -adrenergic signaling, increases mitochondriogenesis, UCP-1 expression and activity as well as the size and number of brown adipocytes resulting in a phenomenon known as cold-induced thermogenesis. The cold-intolerance observed in this study is probably due to a defect in the activation of the brown adipose tissue. Such a defect should also decrease diet-induced thermogenesis and be responsible of the higher food efficiency on HFD, in line with a previous study showing that prenatal nicotine exposure induces long-term alterations in adrenergic responsiveness of sympathetic target tissues (33). Similarly, in mice deficient for the three β -adrenoreceptor subtypes, decreases in cold- and diet-induced thermogenesis led to the development of an obese phenotype (34, 35). Further investigations of the β -adrenergic control of the BAT in prenatally nicotine-exposed animals could help to better understand their phenotype related to impaired thermogenesis.

In conclusion, our work allows an interpretation of the metabolic disorders related to prenatal nicotine exposure. In fact, nicotine, at levels that are relevant for human exposure, induces an atrophy of the endocrine pancreas and a stimulation of white adipose tissue development in pups before weaning. Surprisingly, despite these alterations occurring at an early stage of development in the pancreatic islets, insulin secretion at adulthood is sustained and can even be increased above the level observed in control rats during a glucose challenge.

We conclude that these early alterations in the pancreas might be due to a direct effect of fetal toxicity. The main secondary effects of fetal nicotine exposure shown in this study are the marked high amount of fat storage in the white adipose tissue which is not due to an increase in food intake but rather to a reduced spontaneous physical activity and a deficient thermogenesis activation by cold exposure and probably also in response to a high fat diet. The increased fat accretion in different white adipose tissue depots might contribute to the insulin resistance demonstrated in the present study with clearly pathological glucose and insulin tolerance tests at adult age. An increase in body fat mass is known to induce the metabolic syndrome and in particular insulin resistance (36, 37, 38). In consequence, this study indicates that smoking as well as nicotine replacement during pregnancy might be responsible for childhood obesity and for metabolic disorders later in life in the offspring.

Acknowledgment

This work was supported by a grant from the Swiss National Science Foundation targeted National Research Program 50 "Endocrine disruptors: relevance to humans, animals and ecosystems" grants to Pr Michel Aubert and Pr Petra Hüppi. Pr Petra Hüppi is also supported by the Novartis Foundation. We acknowledge the excellent technical assistance of Audrey Toulotte and the help of Dr Alexandra Chatagner and Dr Pierre Larvaron for some *in vivo* experiments and of Mary Hochstrasser for manuscript language correction. We are grateful to Dr Christelle Veyrat-Durebex and Pr Françoise Rohner-Jeanrenaud from the Small Animal Phenotyping Facility (CMU, University of Geneva, Geneva) for the calorimetry and physical activity measurements and to Pr Paolo Meda, Anne Charollais and Dorothée Caille for the pancreatic islets isolation method teaching. We are grateful to Pr Kenneth Shroyer for the gift of survivin antibody. The authors confirm the absence of any conflict of interest. E.S. and V.M.S contributed equally to this work.

REFERENCES

1. **Gluckman PD, Hanson MA** 2004 The developmental origins of the metabolic syndrome. *Trends Endocrinol Metab* 15:183-7
2. **Hales CN, Barker DJ** 1992 Type 2 (non-insulin-dependent) diabetes mellitus: the thrifty phenotype hypothesis. *Diabetologia* 35:595-601
3. **Vickers MH, Breier BH, Cutfield WS, Hofman PL, Gluckman PD** 2000 Fetal origins of hyperphagia, obesity, and hypertension and postnatal amplification by hypercaloric nutrition. *Am J Physiol Endocrinol Metab* 279:E83-7
4. **Shiverick KT, Salafia C** 1999 Cigarette smoking and pregnancy I: ovarian, uterine and placental effects. *Placenta* 20:265-72
5. **Robinson JS, Moore VM, Owens JA, McMillen IC** 2000 Origins of fetal growth restriction. *Eur J Obstet Gynecol Reprod Biol* 92:13-9
6. **Williams CM, Kanagasabai T** 1984 Maternal adipose tissue response to nicotine administration in the pregnant rat: effects on fetal body fat and cellularity. *Br J Nutr* 51:7-13
7. **Power C, Jefferis BJ** 2002 Fetal environment and subsequent obesity: a study of maternal smoking. *Int J Epidemiol* 31:413-9
8. **Oken E, Huh SY, Taveras EM, Rich-Edwards JW, Gillman MW** 2005 Associations of maternal prenatal smoking with child adiposity and blood pressure. *Obes Res* 13:2021-8
9. **Gao YJ, Holloway AC, Zeng ZH, Lim GE, Petrik JJ, Foster WG, Lee RM** 2005 Prenatal exposure to nicotine causes postnatal obesity and altered perivascular adipose tissue function. *Obes Res* 13:687-92
10. **Holloway AC, Lim GE, Petrik JJ, Foster WG, Morrison KM, Gerstein HC** 2005 Fetal and neonatal exposure to nicotine in Wistar rats results in increased beta cell apoptosis at birth and postnatal endocrine and metabolic changes associated with type 2 diabetes. *Diabetologia* 48:2661-6
11. **Bruin JE, Kellenberger LD, Gerstein HC, Morrison KM, Holloway AC** 2007 Fetal and neonatal nicotine exposure and postnatal glucose homeostasis: identifying critical windows of exposure. *J Endocrinol* 194:171-8
12. **Levin ED** 2005 Fetal nicotinic overload, blunted sympathetic responsivity, and obesity. *Birth Defects Res A Clin Mol Teratol* 73:481-4
13. **Gao N, White P, Doliba N, Golson ML, Matschinsky FM, Kaestner KH** 2007 Foxa2 controls vesicle docking and insulin secretion in mature Beta cells. *Cell Metab* 6:267-79
14. **Montgomery SM, Ekblom A** 2002 Smoking during pregnancy and diabetes mellitus in a British longitudinal birth cohort. *Bmj* 324:26-7
15. **de Weerd S, Thomas CM, Kuster JE, Cikot RJ, Steegers EA** 2002 Variation of serum and urine cotinine in passive and active smokers and applicability in preconceptional smoking cessation counseling. *Environ Res* 90:119-24
16. **Hackman R, Kapur B, Koren G** 1999 Use of the nicotine patch by pregnant women. *N Engl J Med* 341:1700
17. **Bruin JE, Lehman MA, Gerstein HC, Holloway AC** 2007 Mechanism of Increased Beta Cell Apoptosis at Birth in Rats with Maternal Nicotine Exposure 89TH Annual Meeting ENDO07 TORONTO JUNE 2-5
18. **Bruin JE, Petre MA, Lehman MA, Raha S, Gerstein HC, Morrison KM, Holloway AC** 2008 Maternal nicotine exposure increases oxidative stress in the offspring. *Free Radic Biol Med*

19. **Bruin J, Gerstein H, Morrison K, Holloway AC** 2008 Increased pancreatic beta cell apoptosis following fetal and neonatal exposure to nicotine is mediated via the mitochondria. *Toxicol Sci*
20. **Liggins C, Orlicky DJ, Bloomquist LA, Gianani R** 2003 Developmentally regulated expression of Survivin in human pancreatic islets. *Pediatr Dev Pathol* 6:392-7
21. **Dasgupta P, Kinkade R, Joshi B, Decook C, Haura E, Chellappan S** 2006 Nicotine inhibits apoptosis induced by chemotherapeutic drugs by up-regulating XIAP and survivin. *Proc Natl Acad Sci U S A* 103:6332-7
22. **Xu J, Huang H, Pan C, Zhang B, Liu X, Zhang L** 2007 Nicotine inhibits apoptosis induced by cisplatin in human oral cancer cells. *Int J Oral Maxillofac Surg* 36:739-44
23. **Butler AE, Janson J, Bonner-Weir S, Ritzel R, Rizza RA, Butler PC** 2003 Beta-cell deficit and increased beta-cell apoptosis in humans with type 2 diabetes. *Diabetes* 52:102-10
24. **Amoruso A, Bardelli C, Gunella G, Fresu LG, Ferrero V, Brunelleschi S** 2007 Quantification of PPAR-gamma protein in monocyte/macrophages from healthy smokers and non-smokers: a possible direct effect of nicotine. *Life Sci* 81:906-15
25. **Li MD, Parker SL, Kane JK** 2000 Regulation of feeding-associated peptides and receptors by nicotine. *Mol Neurobiol* 22:143-65
26. **Toschke AM, Ehlin AG, von Kries R, Ekblom A, Montgomery SM** 2003 Maternal smoking during pregnancy and appetite control in offspring. *J Perinat Med* 31:251-6
27. **LeSage MG, Gustaf E, Dufek MB, Pentel PR** 2006 Effects of maternal intravenous nicotine administration on locomotor behavior in pre-weanling rats. *Pharmacol Biochem Behav* 85:575-83
28. **Eppolito AK, Smith RF** 2006 Long-term behavioral and developmental consequences of pre- and perinatal nicotine. *Pharmacol Biochem Behav* 85:835-41
29. **Oliff HS, Gallardo KA** 1999 The effect of nicotine on developing brain catecholamine systems. *Front Biosci* 4:D883-97
30. **Turnbaugh PJ, Ley RE, Mahowald MA, Magrini V, Mardis ER, Gordon JI** 2006 An obesity-associated gut microbiome with increased capacity for energy harvest. *Nature* 444:1027-31
31. **Turnbaugh PJ, Backhed F, Fulton L, Gordon JI** 2008 Diet-induced obesity is linked to marked but reversible alterations in the mouse distal gut microbiome. *Cell Host Microbe* 3:213-23
32. **Cannon B, Nedergaard J** 1985 The biochemistry of an inefficient tissue: brown adipose tissue. *Essays Biochem* 20:110-64
33. **Navarro HA, Mills E, Seidler FJ, Baker FE, Lappi SE, Tayyeb MI, Spencer JR, Slotkin TA** 1990 Prenatal nicotine exposure impairs beta-adrenergic function: persistent chronotropic subsensitivity despite recovery from deficits in receptor binding. *Brain Res Bull* 25:233-7
34. **Jimenez M, Leger B, Canola K, Lehr L, Arboit P, Seydoux J, Russell AP, Giacobino JP, Muzzin P, Preitner F** 2002 Beta(1)/beta(2)/beta(3)-adrenoceptor knockout mice are obese and cold-sensitive but have normal lipolytic responses to fasting. *FEBS Lett* 530:37-40
35. **Asensio C, Jimenez M, Kuhne F, Rohner-Jeanrenaud F, Muzzin P** 2005 The lack of beta-adrenoceptors results in enhanced insulin sensitivity in mice exhibiting increased adiposity and glucose intolerance. *Diabetes* 54:3490-5
36. **Boden G, Chen X, DeSantis RA, Kendrick Z** 1993 Effects of age and body fat on insulin resistance in healthy men. *Diabetes Care* 16:728-33
37. **Carey DG, Jenkins AB, Campbell LV, Freund J, Chisholm DJ** 1996 Abdominal fat and insulin resistance in normal and overweight women: Direct measurements

reveal a strong relationship in subjects at both low and high risk of NIDDM. Diabetes 45:633-8

- 38. Gautier JF, Mourier A, de Kerviler E, Tarentola A, Bigard AX, Villette JM, Guezennec CY, Cathelineau G** 1998 Evaluation of abdominal fat distribution in noninsulin-dependent diabetes mellitus: relationship to insulin resistance. J Clin Endocrinol Metab 83:1306-11

Figure Legends

Figure 1

Relevant circulating nicotine metabolite levels in our rodent model of prenatal nicotine exposure

Circulating nicotine metabolite levels (in ng/ml) in gestating female rats after implantation of a subcutaneous osmotic minipump delivering nicotine or vehicle solution before pump implantation (G1), 24 h after pump implantation (G5) and at the end of gestation (G19) (n=10-20 animals in each group). Note that nicotine metabolite levels are non detectable (N.D) at all time points in control mothers.

Figure 2

Increased body weight and white adipose storage at weaning (PND21) in rats prenatally exposed to nicotine

Body weight at birth (n=132-139 animals in each group) and weaning (n=42-59 animals in each group) (A) and relative weight of organs at weaning expressed as % of body weight (n=9-10 animals in each group) (B) of prenatally nicotine-exposed (■) and control (□) male rats. Some SEMs are not visible in the graph due to their low values. * $p \leq 0.05$ for prenatally nicotine-exposed vs. controls.

Figure 3

Enhanced adipogenesis at weaning (PND21) in rats prenatally exposed to nicotine

Histological sections of eWAT (A), mean area of adipocytes expressed in μm^2 (n=5-6 animals in each group) (B) and mRNA levels (in arbitrary units, A.U) in eWAT (n=9-10 animals in each group) (C) of prenatally nicotine-exposed (■) and control (□) male rats at weaning. * $p \leq 0.05$ for nicotine-exposed vs. controls.

Figure 4

Alteration of endocrine pancreas development at the age of 7 days (PND7) in rats prenatally exposed to nicotine

Morphological analysis of pancreas (n=5-6 animals in each group): islet area reported to whole pancreas area (upper panel), mean islet size expressed in μm^2 (middle panel), number of islets per section (lower panel) (A), mRNA levels in pancreatic islets (in arbitrary units, A.U) (n=6 pools of 3 animals in each group) (B), survivin immunolabeling in pancreatic islets (C) of prenatally nicotine-exposed (■) and control (□) male rats at the age of 7 days. Note the reduced size of islets of prenatally nicotine-exposed rats compared to controls in C. * $p \leq 0.05$ for prenatally nicotine-exposed vs. controls.

Figure 5

Post-weaning metabolic disorders in rats prenatally exposed to nicotine

Body weight curves of prenatally nicotine-exposed and control rats fed either a chow diet or a high fat diet (HFD) once weaned (n=9-10 animals in each group), * $p \leq 0.05$ for prenatally nicotine-exposed vs. controls (both group on chow once weaned), # $p \leq 0.05$ for prenatally nicotine-exposed vs. control (both group on HFD once weaned) (A). Cumulative energy intake (in kcal) of these animals from 4-18 weeks of life (n=9-10 animals in each group), * $p \leq 0.05$ for HFD vs. chow (as well as for control as prenatally nicotine-exposed) (B). Food efficiency of these animals (expressed as grams of food ingested to induce 1 gram body weight gain in 14 weeks) (n=9-10 animals in each group), * $p \leq 0.02$ for prenatally nicotine-exposed on HFD vs. controls on HFD (C). Delta rectal temperature (expressed in $^{\circ}\text{C}$) after short-term cold-exposure (6 h at 4°C) at the age of 15 weeks in prenatally nicotine-exposed (●) and control (○) males rats fed a chow diet once weaned (n=10-12 animals in each group) (D). Voluntary ambulatory activity (expressed in a thousand counts per period) at the age of 18 weeks during light and dark phase of prenatally nicotine-exposed (■) and control (□) male rats (n=5-6 animals in each group), * $p \leq 0.05$ for prenatally nicotine-exposed vs. controls (E).

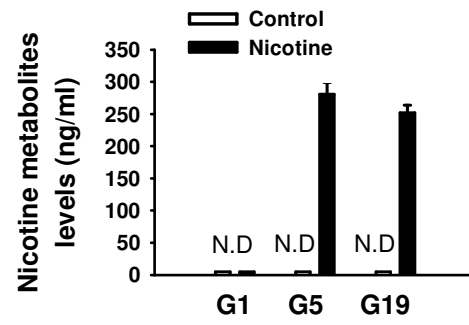
Figure 6

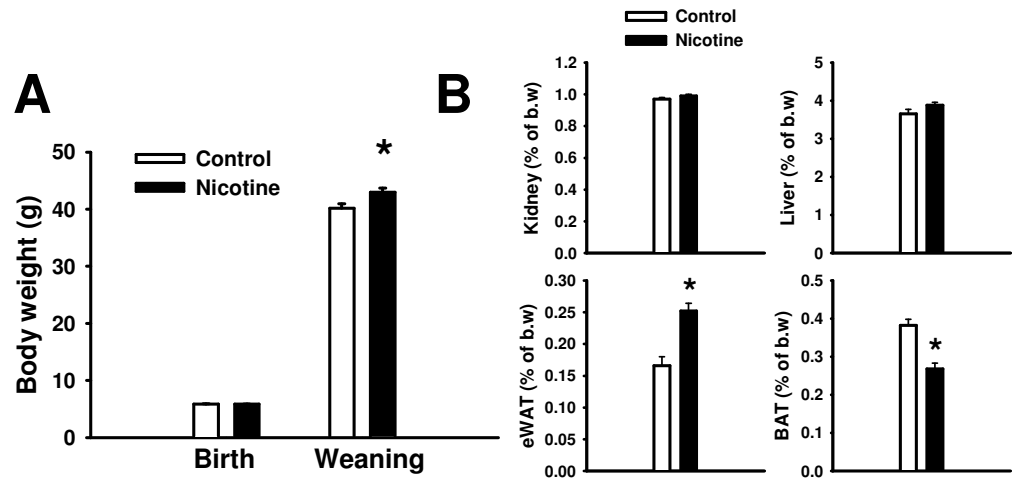
Alteration of glucose homeostasis and insulin sensitivity in rats prenatally exposed to nicotine

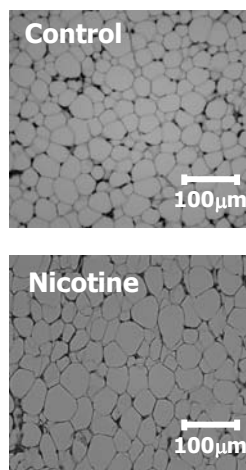
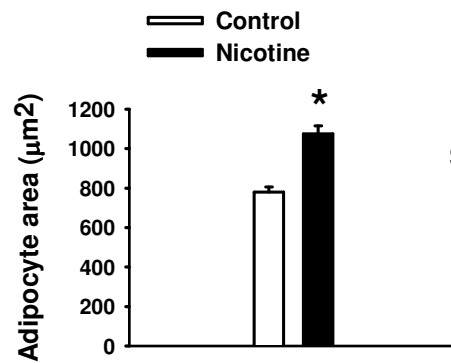
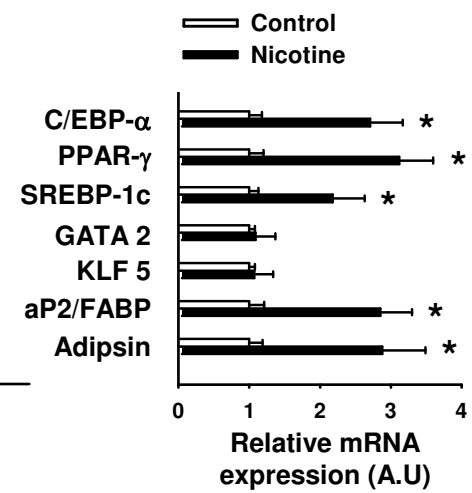
Blood glucose levels (in mmol/l) during glucose tolerance test (A), blood insulin levels (in ng/ml) during the same glucose tolerance test (B), blood glucose levels (in mmol/l) during insulin tolerance test (C) of prenatally nicotine-exposed (●) and control (○) male rats at the age of 26 weeks. n=7-9 animals in each group for all panel. * $p \leq 0.05$ for prenatally nicotine-exposed vs. controls.

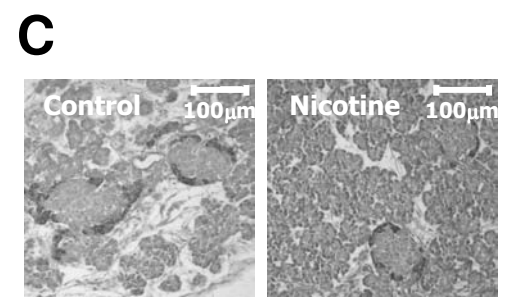
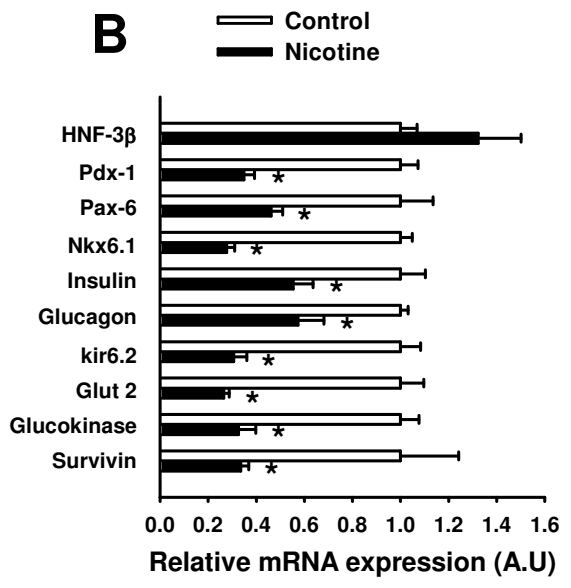
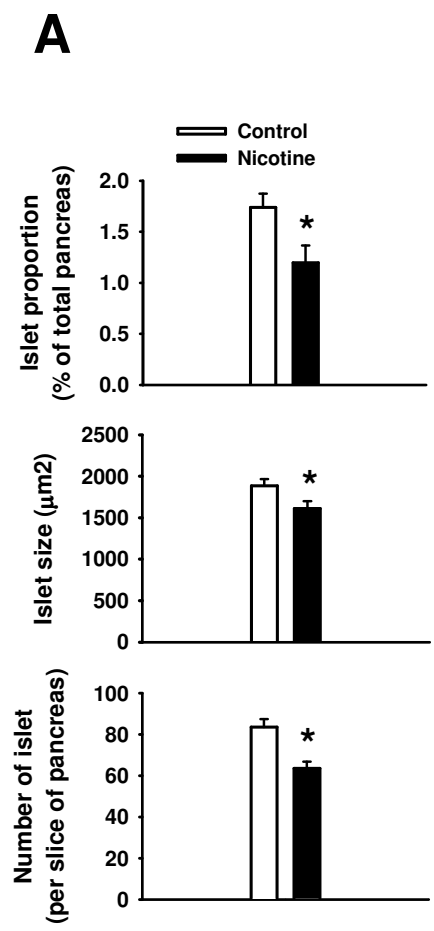
TABLE 1. PCR primers for quantitative real-time PCR

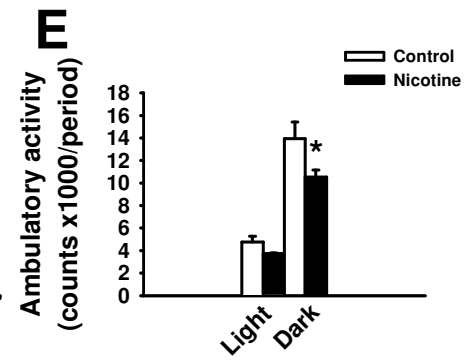
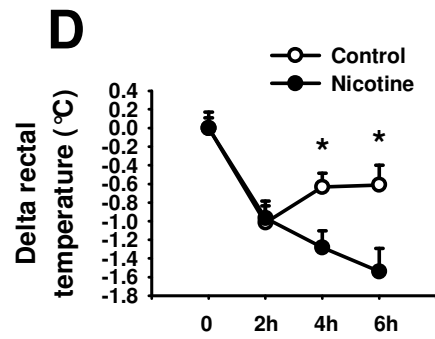
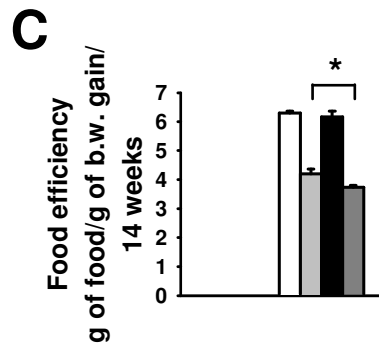
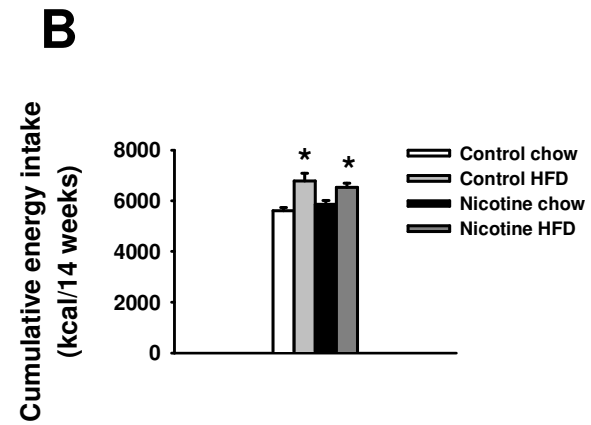
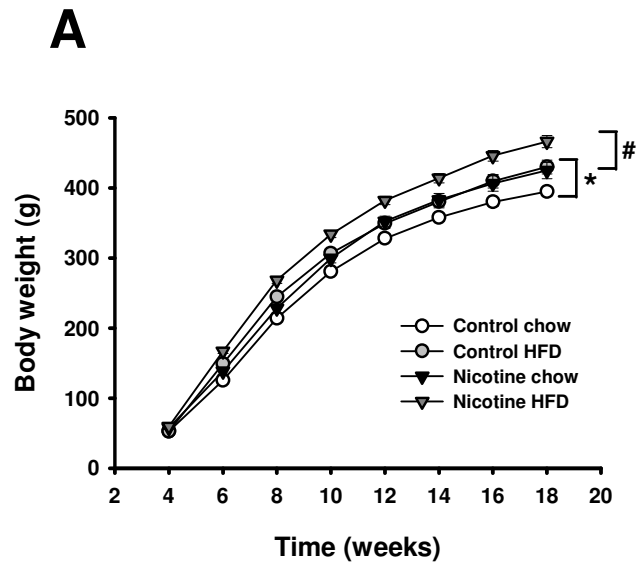
	Forward	Reverse
C/EBP- α	5'-AGTTGACCAGTGACAATGACCG-3'	5'-TCAGGCAGCTGGCGGAAGAT-3'
PPAR- γ	5'-CTGACCCAATGGTTGCTGATTAC-3'	5'-GGACGCAGGCTCTACTTTGATC-3'
SREBP-1C	5'-CATCGACTACATCCGCTTCTTACA-3'	5'-GTCTTTCAGTGATTTGCTTTTGTGA-3'
GATA-2	5'-AATCGGCCGCTCATCAAG-3'	5'-TCGTCTGACAATTTGCACAACA-3'
KLF5	5'-GTCCGATACAACAGAAGGAGTAACC-3'	5'-ACTTTTGTGCAACCATCATAATCAC-3'
aP2	5'-TGATTACATGAAAGAAGTGGGAGTTG-3'	5'-CAAGTTGGGCTTGGCCATA-3'
Adipsin	5'-CATGGATGGAGTGACCAAGGA-3'	5'-CACTTTCACATCATACAAATGCTT-3'
LPL	5'-ACAGTCTTGGAGCCCATGCT-3'	5'-AGCCAGTAATTCTATTGACCTTCTGT-3'
HNF-3 β	5'-CATCCGACTGGAGCAGCTACT-3'	5'-CCCAGGCTGGCGTTCAT-3'
Pdx-1	5'-CCGCGTTCATCTCCCTT-3'	5'-CTCCTGCCCACTGGCTTTT-3'
Pax-6	5'-CCAACGACAATATACCCAGTGTGT-3'	5'-GCGCCCATCTGTTGCTTTT-3'
Nkx6.1	5'-CCCCATCAAGGATCCATT-3'	5'-CTGCTGGCCGGAGAATGT-3'
Insulin	5'-CAGCACCTTTGTGGTCCTCA-3'	5'-CCCACACACCAGGTACAGAGC-3'
Glucagon	5'-CGCCGTGCTCAAGATTTTGT-3'	5'-CCGGTTCCTCTTGGTGTTCAT-3'
Kir6.2	5'-GCCCTGCGTCACAAGCA-3'	5'-GCACCTCGATGGAGAAAAGGA-3'
Glut 2	5'-TCACAGGCATTCTTATTAGTCAGATTG-3'	5'-AGTAGGATGTGCCAGTAATCCTGAT-3'
glucokinase	5'-CACCCCAGAAGGCTCAGAAG-3'	5'-AGCATCACTCTGAAGTTGGTTCCT-3'
Survivin	5'-GGCTTTTATTACCGGGACACAGT-3'	5'-CCAGCATCTTAGCCACCAT-3'
36B4	5'-TTCCCACTGGCTGAAAAGGT-3'	5'-CGCAGCCGCAAATGC-3'

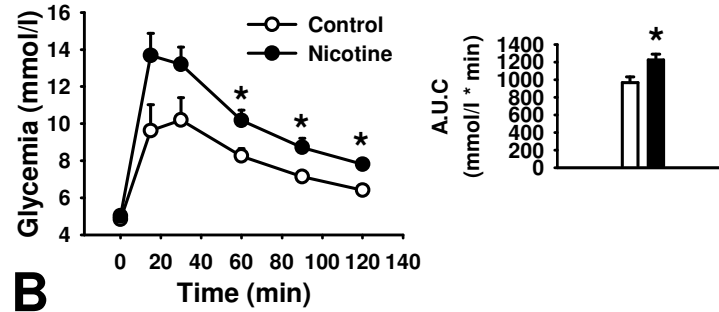
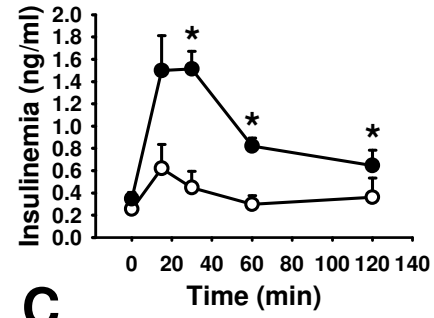




A**B****C**





A**B****C**